The Influence of Biodegradability and Inoculum-to-Substrate Ratio on the Anaerobic Digestion Performance and Microbial Diversity

Article *in* GCB Bioenergy · November 2025

DOI: 10.1111/gcbb.70090

CITATIONS
0

READS
16

9 authors, including:

Marvin T. Valentin
Wrocław University of Environmental and Life Sciences
25 PUBLICATIONS **186** CITATIONS
SEE PROFILE

Agata Siedlecka
Wrocław University of Environmental and Life Sciences
22 PUBLICATIONS **166** CITATIONS
SEE PROFILE

Kacper Świechowski
Wrocław University of Environmental and Life Sciences
41 PUBLICATIONS **523** CITATIONS
SEE PROFILE

Vitalii Demeshkant
Wrocław University of Environmental and Life Sciences
16 PUBLICATIONS **58** CITATIONS
SEE PROFILE

GCB Bioenergy

WILEY

Global Change Biology Bioenergy
BIOPRODUCTS FOR A SUSTAINABLE BIOECONOMY

RESEARCH ARTICLE OPEN ACCESS

The Influence of Biodegradability and Inoculum-to-Substrate Ratio on the Anaerobic Digestion Performance and Microbial Diversity

Marvin T. Valentin[1,2,3] | Katarzyna Ewa Kosiorowska[1] | Agata Siedlecka[1] | Kacper Świechowski[1] | Vitalii Demeshkant[4] | Paweł Wiercik[5] | Svetlana Ashikhmina[1] | Tomasz Strzała[6] | Andrzej Białowiec[1]

[1]Department of Applied Bioeconomy, Wrocław University of Environmental and Life Sciences, Wroclaw, Poland | [2]Department of Agricultural and Biosystems Engineering, College of Engineering, Benguet State University, La Trinidad, Benguet, Philippines | [3]Engineering and Industrial Research, Department of Science and Technology, National Research Council of the Philippines, Taguig, Philippines | [4]Laboratory of Electron Microscopy, Institute of Biology, Wrocław University of Environmental and Life Sciences, Wroclaw, Poland | [5]The Faculty of Environmental Engineering and Geodesy, Institute of Environmental Engineering, Wrocław University of Environmental and Life Sciences, Wrocław, Poland | [6]Faculty of Biology and Animal Science, Department of Genetics, Wrocław University of Environmental and Life Sciences, Wroclaw, Poland

Correspondence: Andrzej Białowiec (andrzej.bialowiec@upwr.edu.pl)

Received: 26 April 2025 | **Revised:** 13 September 2025 | **Accepted:** 27 September 2025

Funding: This work (without the BC part) was supported by the Wrocław University of Environmental and Life Sciences under the Innovative grant with Agreement No. N0N00000/0241/41/2023. This part of the research regarding the application of biochar was funded by the National Science Centre, Poland, grant number UMO-2021/43/B/ST8/01924. For Open Access, the author has applied a CC-BY public copyright license to any Author Accepted Manuscript (AAM) version arising from this submission. The APC is financed by Wrocław University of Environmental and Life Sciences.

Keywords: biochar | biodegradability | biomethane | gene sequencing | inoculum-to-substrate ratio | SEM

ABSTRACT

Continuous-flow anaerobic digestion (AD) of wheat straw (WS) is often limited by volatile fatty acid (VFA) accumulation at low inoculum-to-substrate ratios (ISRs). Here, biochar (8.0 g/L) recovered methane production in overloaded systems (ISR 0.5, HRT 12 days), increasing yields by 658.45 mL/g-VS. Microbial analysis revealed a shift from *Methanomicrobiaceae* to *Methanosarcinaceae* dominance upon biochar addition, correlating with *mcr*A gene upregulation. This strategy enhances the AD of refractory feedstocks without diluting the organic load. The results offer insights into optimizing biogas systems treating low-biodegradability feedstocks at low ISRs, highlighting biochar's potential to stabilize performance and enrich functional microbial communities under stress conditions.

1 | Introduction

Anaerobic digestion (AD) provides sustainable and environmentally friendly solutions for treating various organic wastes (Molatudi et al. 2025). However, it is estimated that even up to 70%–90% of digestate remains undigested (Czekała et al. 2022; Romio et al. 2022), pointing to inefficiencies in the AD process that are often linked to the biodegradability of the substrate. Highly biodegradable materials, such as glucose, degrade rapidly and may cause excessive volatile fatty acids (VFAs) accumulation, leading to process inhibition (Cai et al. 2016). Conversely, hardly biodegradable substrates like lignocellulosic biomass (e.g., wheat straw [WS]) are resistant to microbial breakdown due to their complex chemical structure composed of cellulose, hemicellulose, and lignin (van Meerbeek et al. 2014; Liu et al. 2019). These differences necessitate tailored operational strategies, including substrate pretreatment and careful adjustment of the inoculum-to-substrate ratio (ISR). Among these strategies, the interaction between ISR and biochar supplementation in continuous systems remains poorly understood.

ISR represents the proportion of the inoculum and substrate in the reactor. The inoculum is a nutrient-rich digestate sourced from an existing successful reactor to start the process of the new AD. It is an important parameter affecting biodegradability and is linked to the hydrolysis rate and methane production (Johnravindar et al. 2022). Although the influence of ISR on the AD process has been widely studied using batch experiments (Valentin and Białowiec 2024a), recent papers presenting results of research conducted on lab-scale continuous-flow anaerobic digestion (CFAD) at different ISRs remain scarce. This knowledge gap is particularly critical for understanding ISR–microbiome interactions in continuous-flow systems. Nevertheless, it can be assumed that low ISRs improve yields, but pose a risk of instability in CFAD, due to increased organic loading rate (OLR) (Elliott et al. 2024).

The potential of biochar to address ISR-related instability has gained attention in recent studies. While proper ISR management can address some challenges associated with substrate biodegradability, additional interventions, such as biochar (BC) supplementation, may further enhance system stability and performance. For example, Ngo et al. (2024) claimed that semi-continuous reactors treating chicken manure exhibited an 8.4-fold improvement in methane production (demonstrating increased chemical oxygen demand removal and maintaining lower total ammonia concentrations at the same time) with BC supplementation, compared to control reactors. Similar findings were presented by Zhang et al. (2024) who stated that BC increased methane yield in anaerobic membrane bioreactor treating ammonia-rich swine wastewater by enriching *Syntrophomonas* and *Methanosarcina/Methanospirillum* under ammonia stress. Furthermore, Shao et al. (2025) introduced magnetic BC into semi-continuous AD of substrates with various C/N ratios, observing alleviated acid inhibition and mitigation of ammonia accumulation in the carbon- and ammonia-rich reactors, respectively. Noteworthy, magnetic BC promoted the hydrogenotrophic methanogenesis pathway in carbon-rich reactors, whereas acetoclastic methanogenesis was enhanced in ammonia-rich reactors.

Interestingly, Wambugu et al. (2019) found that during AD of food waste (FW), the biogas volume produced by the treatments with BC supplementation was lower than that produced by the control reactors in batch experiments; however, BC enhanced the AD performance of a continuous upflow anaerobic sludge blanket reactor. The reasons behind these observations require further research. Particularly, the role of biochar under different ISR conditions in continuous systems needs clarification. On the other hand, Elliot et al. reported that in the BC-amended, bench-scale semi-continuous AD of high-strength source-separated industrial wastewaters, maintained at ISR 3.5, biogas yields were lower than expected, while stability was possible at high hydraulic retention times (HRTs) (30 and 45 days) (Elliott et al. 2024). In the mentioned study, *Methanosarcina* was linked to the increased biomethane production.

Despite increasing interest in carbon materials-amended CFAD, the role of BC in microbial dynamics, especially of hardly biodegradable biomass at low ISRs, remains unresolved. Based on the literature review, however, one can hypothesize that BC could act as a factor enriching stress-tolerant *Methanosarcinaceae* under prone-to-instability conditions of low ISR, thus restoring biomethane production. This hypothesis is particularly relevant for continuous systems where low ISR operation is economically favorable but operationally challenging.

To fill the existing knowledge gap, in the current study, substrates with varying biodegradability—glucose (high), FW (medium), and WS (low)—were used under different influent ISR (2.0 and 0.5), and BC was supplemented close to the end of the experiment. Beyond biomethane production, other parameters, like VFA concentrations, methyl-coenzyme M reductase (*mcr*A) gene copy numbers, and microbial shifts, were monitored throughout the experiment to better demonstrate the ISR-BC-microbiome nexus in CFAD.

2 | Materials and Methods

2.1 | Substrates, Inoculum, and Biochar

Glucose (GL), FW, and WS were used as substrates. The major components of simulated FW were vegetables (31.2%), bread (23%), meat (15%) (den Boer et al. 2023), fruits (24.8%), and others, including rice (4%) (Nagao et al. 2012). The fresh FW was dried at 105°C for 24 h and underwent size reduction by grinding and screening to particles below 1.0 mm. After the size reduction, the FW was homogenized in a stainless-steel blender and stored in a freezer until further use (Chakraborty et al. 2022). Glucose (Geyer, Poland) was used without further modification. A quantity of air-dried WS was ground using an electrical stainless-steel grinding machine to a particle size of < 2.0 mm. The inoculum was acquired from an agricultural biogas plant that treats FW and farming residues (mostly potatoes and sugar beets) and was processed as described previously (Valentin et al. 2023). Wood biochar (BC) pyrolyzed at 500°C for 120 min was used (8.0 g/L) as a supplement on days 76 to 95 of the experiment, during the shortened HRT.

2.2 | Anaerobic Digestion Test

The experiment was performed in two types of reactors. First, the AD was done using batch reactors to measure the biomethane potential and substrate biodegradability. Next, the AD process was performed in a continuous-flow reactor setup to study the influence of ISR and HRT on biomethane production from the AD of the substrates with different biodegradability (Figure 1).

In the batch experiment, an automatic methane potential test system (AMPTS) (BPC Instruments AB, Lund, Sweden) with 15 reactors (500 mL) was used with a working volume of 400 mL. The ISR were 2.0 and 0.5. ISR 2.0 is considered to provide optimal conditions for microorganisms, while ISR 0.5 is deemed to contain high organic material that may result in process disturbance (IEA Bioenergy 2018). The produced biomethane was automatically measured and recorded. The biomethane generated from the AD of the substrates was obtained by subtracting the amount of biomethane produced by the inoculum from the total biomethane produced by the mixture of the substrate and inoculum (Valentin et al. 2023). To understand the

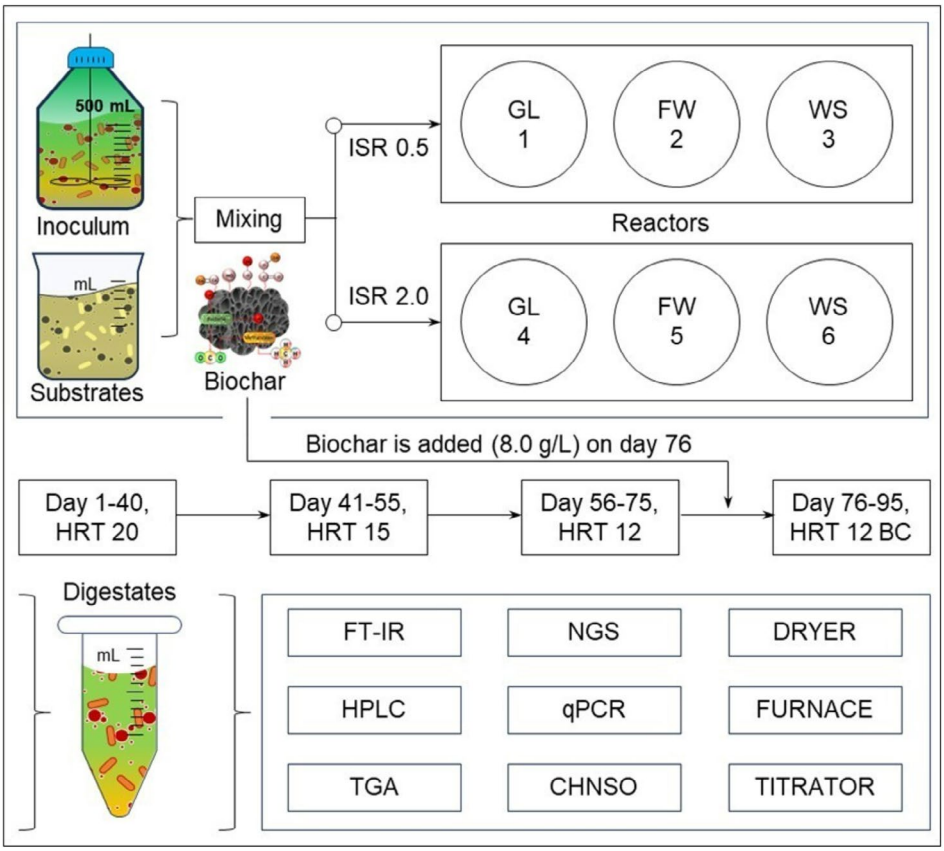

FIGURE 1 | Flow chart of the experiment.

kinetics of biomethane production, the BMP was fitted into the Modified Gompertz model discussed in previous studies (Namal 2020; Valentin and Białowiec 2024b). The biodegradability expressed as the biomethane production constant rate, k (d^{-1}), of the substrates obtained from the Gompertz model, and the specific biomethane production was modeled in a quadratic fit using the Statistica Software described above. The k values were calculated by dividing R_{max} by P. The statistical parameters of the models were assessed in terms of the root mean square error (RMSE) (Nguyen et al. 2019), coefficient of determination (R^2) (Pererva et al. 2020), and mean absolute deviation (MAD). The theoretical biomethane potential (TBMP) mL/g-VS of the substrates was estimated using the Buswell and Mueller stoichiometric formulas (Buswell and Mueller 1952).

The continuous-flow experiment was conducted in bioprocess control (BPC) with 6 identical reactors. Each reactor had a total volume of 2.0 L, and the working volume was set to 1.8 L. The reactors were initially filled with inoculum and were fed daily with a mixture of substrate and new inoculum. Reactors 1, 2, and 3 were maintained at ISR2.0 and were labeled GL2, FW2, and WS2, representing variants with glucose, FW, and WS, respectively. Reactors 4, 5, and 6 were maintained at ISR0.5 and were labeled GL0.5, FW0.5, and WS0.5, representing variants with glucose, FW, and WS, respectively. The experiment commenced with a HRT set at 20 days, achieved by introducing an influent of 90 mL/day for 40 days. Subsequently, from day 41 to 55, the HRT was shortened to 15 days, corresponding to an increased feeding rate of 120 mL/day. From day 56 until the end of the experiment, the feeding rate was increased to reach a 12-day HRT equivalent to a volumetric feed rate of 150 mL/day (Table 1). At GL2.0 and GL0.5, the OLR were 1.42 and 5.38 g-VS/day, respectively. Similarly, FW2.0 and FW0.5 had OLR values of 1.39 and 4.91 g-VS/day, while WS2.0 and WS0.5 had OLR values of 1.36 and 4.60 g-VS/day, respectively. At the onset of day 76, BC was introduced into the influent (8.0 g/L) (Valentin and Białowiec 2024b).

2.3 | Analytical Method

The TS, VS, VM, and AC of the feedstock, biochar, inoculum, and digestate samples were determined in a thermogravimetric analyzer (TGA) (Mettler Toledo) (Torquato et al. 2017). The thermal decomposition of the BC and digestates was determined under a nitrogen atmosphere (50 mL/L). The temperature ranged from 30°C to 950°C at a 10°C/min heating rate. An aluminum oxide crucible (70 μL) was used. The fixed carbon was obtained by FC = 100−VM−AC (Pulgarín-Muñoz et al. 2025). The C, H, N, and S were measured with the use of an elemental analyzer (PerkinElmer, 2400 CHNS/O Series II, Waltham, MA, USA). On that basis, the carbon-relative molar mass of the materials was calculated (Białowieca and Syguła 2025). The pH values of the BC and substrates were measured at a ratio of 1:20 (w/v) in water after being shaken for 24 h at 130 rpm (Zheng et al. 2013).

The functional groups were analyzed using a Thermo Scientific Nicolet iZ10 FT-IR spectrometer, a module of the Nicolet iN10

TABLE 1 | Matrix of the continuous-flow experiment.

			Phases										
			1 to 40 days			41 to 55 days			56 to 75 days			76 to 95 days	
ISR	Substrate	Label	HRT	OLR	BC	HRT	OLR	BC	HRT	OLR	BC	HRT	OLR	BC
2.0	Glucose	GL2	20	0.85	0	15	1.14	0	12	1.42	0	12	1.42	8.0
2.0	Food waste	FW2	20	0.83	0	15	1.11	0	12	1.39	0	12	1.39	8.0
2.0	Wheat straw	WS2	20	0.82	0	15	1.09	0	12	1.36	0	12	1.36	8.0
0.5	Glucose	GL0.5	20	3.23	0	15	4.30	0	12	5.38	0	12	5.38	8.0
0.5	Food waste	FW0.5	20	2.94	0	15	3.92	0	12	4.91	0	12	4.91	8.0
0.5	Wheat straw	WS0.5	20	2.76	0	15	3.68	0	12	4.60	0	12	4.60	8.0

Abbreviations: BC, biochar concentration (g/L); HRT, hydraulic retention time (Days); OLR, organic loading rate (g-VS/Day).

MX microscope, equipped with a Smart iTX accessory featuring a diamond plate. Attenuated Total Reflection–Fourier Transform Infrared (ATR-FTIR) analyses were performed at a spectral resolution of 4 cm^{-1}, with each spectrum representing the average of 32 scans within the 400–4000 cm^{-1} wavenumber range.

The substrates, biochar, inoculum, and digestate from the reactor representing days 55 to 75 (no BC) and from days 76 to 95 (BC phase) were characterized using SEM–EDX. The dried sample specimens were mounted onto aluminum stubs using double-sided carbon tape and coated with gold for 400 s using an ion sputter coater (Edwards Scancoat Six Sputter Coater). The samples were then examined using a scanning electron microscope (Zeiss Evo LS15), with random regions of each specimen analyzed. Scanning electron microscopy (SEM) equipped with a field emission (FE) gun enables high-resolution imaging, providing detailed insights into the three-dimensional ultrastructure of macerated tissues. A semi-quantitative elemental analysis of the BC samples was performed using energy-dispersive X-ray spectrometry (EDX) with a Quantax 200 XFlash detector (Bruker, Berlin, Germany) operating at 20 kV. The detected surface elements were quantified as weight percentages (wt.%), and elemental maps (O, Mg, K, Pb, Si, P, Ca, Fe) were generated to visualize their spatial distribution on the BC surface.

To get a deeper understanding of the process, digestate samples were analyzed for qualitative and quantitative VFA content. Samples were collected at days 0, 5, 20, 40, 47, 55, 60, 65, 70, 76, 81, 87, and 95 and were analyzed for specific VFA contents. Samples taken during the AD were protected by freezing at −20°C and thawed at room temperature before analysis. Defrosted samples were centrifuged at 10°C at 4500 rpm for 10 min. Samples were diluted in Milli-Q water and re-centrifuged at 10°C for 5 min at 15000 rpm. Ultra-Performance Liquid Chromatography (U-HPLC) was used for quantitative and qualitative analysis using the UltiMate 3000 System (ThermoFisher Scientific, UK). The VFA 10 mM standard solution (Volatile Free Acid Mix, CRM46975, Merck, Poland) was used to prepare calibration curves. Standards were stored at 4°C, according to the manufacturer's guidelines. The ethanol standard was purchased from the Geyer company. HyperREZ XPCarbohydrateH+8 μm column (Thermo Scientific, Waltham, MA) and isocratic elution were used to determine the concentration of VFA (and other components such as ethanol). Identification of analytes was performed with the UV/VIS-DAD detector at 208 ± 1 nm, and a refractive index (RI) detector (Shodex, Ogimachi, Japan) was used simultaneously. 0.25 mM trifluoroacetic acid was used as eluent, the flow rate was 1.1 mL/min, and the column temperature was 35°C (isocratic elution). Data analysis was performed using Chromeleon 7.1 Software.

2.4 | Microbial Analysis

2.4.1 | Genomic DNA Extraction

Genomic DNA was extracted from 25 samples in total, collected from the continuous-flow experiment. Precisely, one sample of inoculum and 24 samples from 6 bioreactors were collected in 4 sampling campaigns (representing HRT 20, 15, 12, and 12 with BC supplementation). DNA was extracted using a DNeasy PowerSoil Pro kit (Qiagen), according to the manufacturer's instructions. The quality and concentration of each DNA sample were measured using a NanoDrop (ThermoScientific). The gDNA was then subjected to quantitative PCR (qPCR) and next-generation sequencing (NGS) analyses.

2.4.2 | Real-Time PCR

Real-time PCR (qPCR) was conducted to detect and quantify the *mcr*A gene, known to code methyl-coenzyme M reductase in all methanogens (Aydin et al. 2015), and the 16S rRNA gene, present in all bacteria and archaea (Maeda et al. 2003). For this purpose, the DyNAmo ColorFlash SYBR Green qPCR Kit (ThermoFisher Scientific) was used according to the manufacturer's instructions. All reactions were run in a CFX96 Touch Real-Time PCR Detection System (BIO-RAD). The details of the reactions are presented in the Supporting Informations (Tables S6–S8).

2.4.3 | Next-Generation Sequencing

The bacterial metabarcoding full-length 16S rRNA gene was amplified, and the library was prepared according to the ONT 16S Barcoding Kit 24 V14 protocol. As full-length 16S rRNA primers used in the ONT kit (27F and 1492R) do not amplify archaeal 16S rRNA sequences, we also amplified shorter 16S rRNA gene fragments with primers ARC344f-mod and Arch958R-mod under PCR conditions. Libraries for archaeal 16S rRNA PCR products were prepared using the Native Barcoding Kit 96 V14, according to the producer's manual. Both archaeal and bacterial 16S rRNA fragments were separately pooled, cleaned, and sequenced using Oxford Nanopore Technologies (ONT) MinION sequencer along with R10.4.1 flow cells (50 k reads per sample minimum). Bacterial and archaea ONT raw data were basecalled with the GPU version of Dorado (https://github.com/nanoporetech/dorado) using a super high accuracy (sup) base calling model. Quality control of the reads was analyzed with PycoQC along with MinIONQC and trimmed using Porechop (https://github.com/rrwick/Porechop) along with Chopper, according to quality control results. Finally, a quantitative analysis tool MetONTIIME (QIIME2 long reads implementation) (Matoute et al. 2024), was used for species identification and statistical differential analyses within sequenced metabarcoded samples. The dataset used in the manuscript has been deposited in the NCBI database under accession numbers: SRR33159634-SRR33159658 and SRR33185919-SRR331185943 for bacterial and archaeal samples, respectively.

3 | Results

3.1 | Properties of Materials

The properties of the feedstock, inoculum, and BC are presented in the Supporting Information (Section S1). The physical and chemical properties were assessed through FT-IR, thermal degradation, and elemental distribution.

3.2 | Anaerobic Digestion Experiment

The cumulative BMP of the tested substrates (GL, FW, and WS) from the batch test is shown in Figure 2. At ISR 0.5, the BMP from FW, WS, and GL were 245.1, 228.6, and 86.4 mL/(g-VS), respectively, while at ISR 2.0 they were 298.5, 212.3, and 275.0 mL/(g-VS), respectively. This translates to conversion efficiency, relative to the theoretical biomethane, of 73.70% for GL2.0 and 27.52% for GL0.5, while 49.87% and 53.72% for WS2.0 and WS0.5, respectively.

The kinetic parameters for the fitted cumulative BMP in the Modified Gompertz model shown in Table 2 indicate that the highest predicted biomethane yields were 298.54 mL/(g-VS) for FW2 and 275.04 mL/(g-VS) for GL2. The data for both FW2 and GL2 demonstrated a strong fit with the model, yielding high coefficients of determination of 0.916 and 0.915, respectively. However, reactors under ISR 0.5 showed poor fitting, suggesting

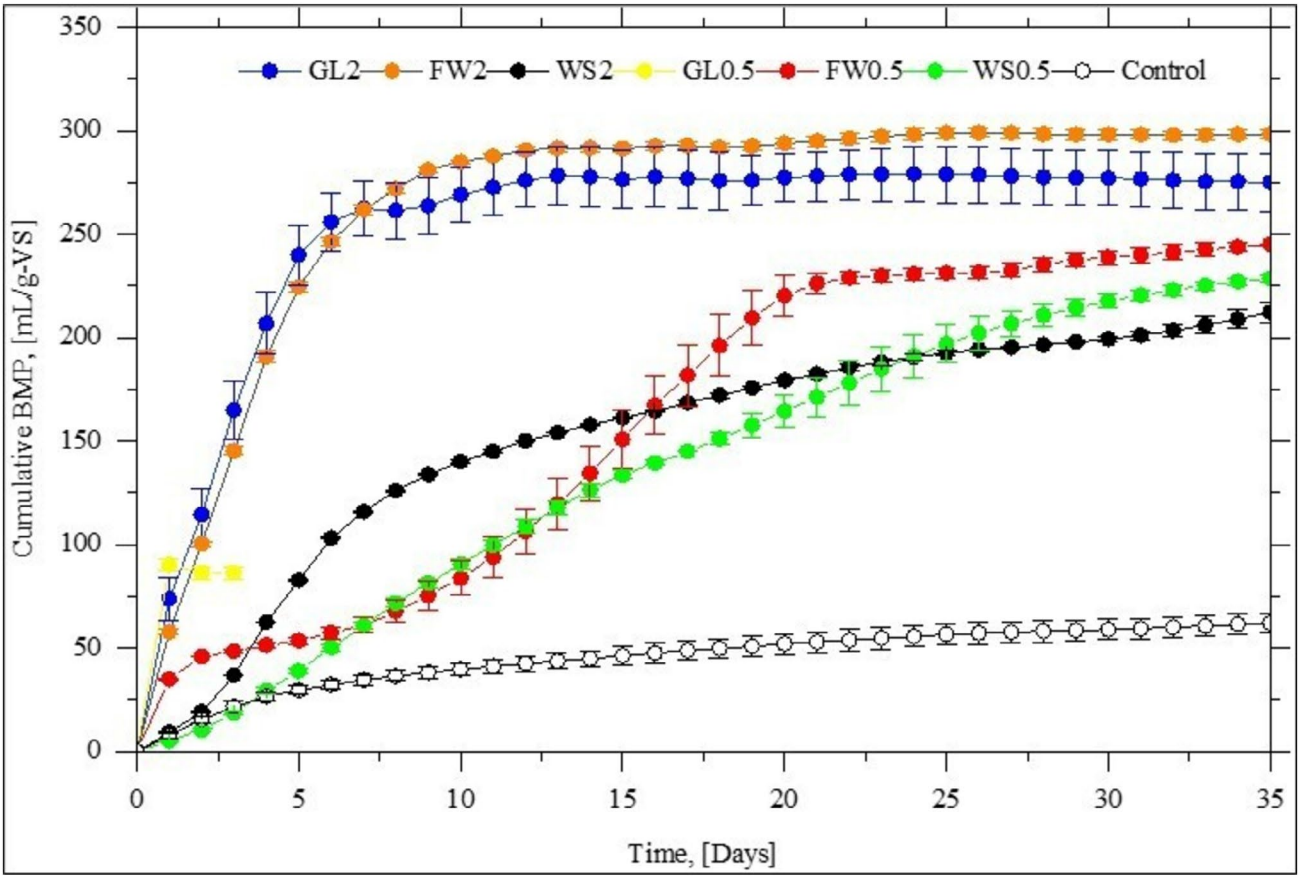

FIGURE 2 | The cumulative biomethane production from the batch test anaerobic digestion of GL-glucose, FW-food waste, and WS-wheat straw at ISR 2.0 and 0.5.

that lower ISRs may introduce variability or inhibition in the system, reducing the model's ability to accurately predict BMP under these conditions.

The specific methane production (SMP) and the daily methane production (DMP) from the AD of the substrates maintained at an ISR of 2.0 and 0.5 for 95 days are shown in Figure 3A,B, respectively. The digestates from the test were analyzed, and the results are presented in the Supporting Informations (Section S2). Overall, the average SMPs of the reactors at ISR2.0 are higher than the group at ISR0.5. During the initial HRT, stabilization period (day 1 to 20), the average SMP from GL2, FW2, and WS2 were 401.74 ± 35.63, 401.70 ± 45.77, and 273.19 ± 51.02 mL/(g-VS), respectively, which are respectively 28.69%, 22.13%, and 44.77% higher than GL0.5, FW0.5, and WS0.5 (Table 2). Analysis of variance shows that average SMPs in the reactors are significantly lower ($p \leq 0.05$) across the HRTs. The least significant difference (LSD) test indicated that SMPs for GL2.0 and FW2.0 are statistically insignificant in all HRTs. The cumulative SMP also shows that

TABLE 2 | The kinetic parameters of the modified Gompertz equation of the predicted biomethane production of glucose, food waste, and wheat straw at ISRs 2.0 and 0.5.

Variants	Predicted BMP, [mL/(g-VS)]	R_{max}, [mL(g-VS/day)]	Lag phase, [day]	RMSE	R^2	Biodegradability (k), [day^{-1}]
GL2.0	277.09	2.23	−0.25	15.63	0.95	0.0080
GL0.5	112.97	0.04	0.0	12.59	0.294	0.0002
FW2.0	295.78	2.00	−0.10	18.66	0.916	0.0068
FW0.5	254.07	0.51	1.74	37.55	0.770	0.0020
WS2.0	193.80	0.61	−0.16	18.91	0.884	0.0031
WS0.5	223.73	0.43	1.54	30.30	0.813	0.0019

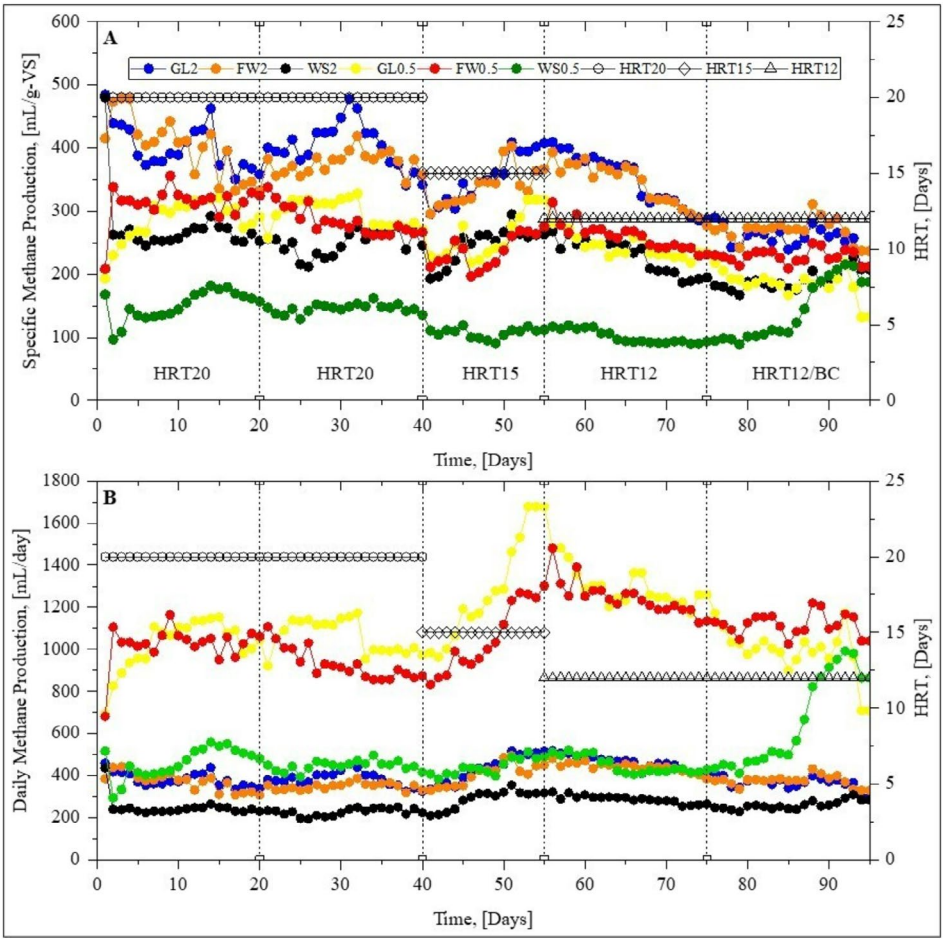

FIGURE 3 | (A) The specific methane production (mL/(g-VS)); and (B) Daily methane production (mL/day) during the AD of GL, WS, and FW at ISR 2.0 and 0.5, and HRTs 20, 15, and 12.

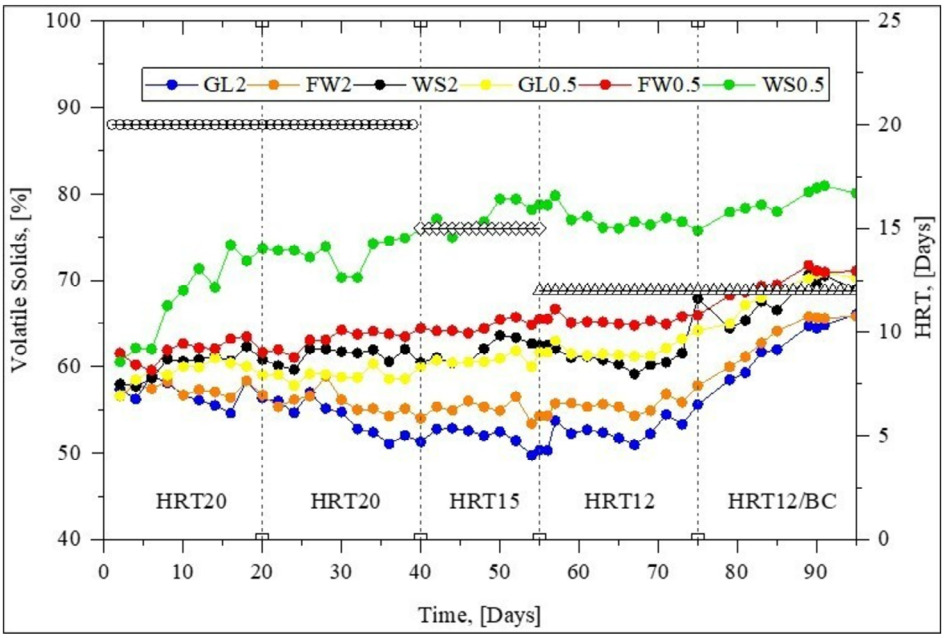

FIGURE 4 | Changes in the volatile solids of the digestate from the anaerobic digestion of glucose, wheat straw, and food waste.

ISR2.0 reactors are higher across the substrates and HRTs (Table S6). The same trend was observed in the succeeding HRTs. A similar result was observed that high ISR increased methane production by ~20% (Xiao et al. 2022). When considering the theoretical BMP, GL2 had the highest average conversion efficiency at 94.57% ± 16.10%, followed by FW2 and GL0.5 at 77.15% ± 11.17% and 68.00% ± 11.81%, respectively. Lower efficiencies at 58.92% ± 7.98%, 55.87% ± 7.21%, and 30.42% ± 5.53% were observed from FW0.5, WS2, and WS0.5, respectively. In the final phase, when BC was added, all reactors, except WS0.5, decreased in the SMP. The average SMP at WS0.5 during the BC phase was 140.70 mL/(g-VS), which is ~40% higher compared to the previous phase (days 56 to 75) under the same HRT with an average SMP of 100.10 mL/(g-VS). Considering the increase in SMP, the BC addition was only effective for WS0.5. The group of reactors at ISRs 0.5 accumulated TVFA. During the BC phase, the TVFA dropped to 11.74 g/L.

In terms of the DMP (Figure 3B), the group of ISR 0.5 reactors is higher than ISR 2.0. On average, GL0.5, FW0.5, and WS0.5 had DMP of 1135.35, 1074.95, and 489.90 mL/day, which are 64.3%, 63.8%, and 46.5% higher than GL2.0, FW2.0, and WS2.0, respectively. Adding BC increased the DMP for WS0.5 at 647.63 mL/day, which is 44% higher than the previous phase at 450.25 mL/day. The highest DMP of 1297.30 mL/day was observed at GL0.5 at HRT 12 (days 56 to 75) but it decreased to 1120.31 mL/day during the BC addition. A similar observation was reported from the AD of grass silage that showed methane yield decreased at higher loading (ISR 0.53) (Benito and Greger 2017).

Figure 4 shows the changes in the VS of the digestate from the reactors. WS0.5 had the highest VS among the reactors, indicating the high amount of organic matter in the digestate, which was not degraded. This explains the low biomethane production in WS0.5. GL2.0 and FW2.0 are lower in VS concentration, ascribed to the lower concentration and high substrate biodegradability.

The highly biodegradable substrates like GL and FW are susceptible to fast accumulation of VFA (Cai et al. 2016). The WS has TVFA below the inhibition limit, allowing the microorganisms to degrade the substrate continuously. The same substrates and ISRs were verified in a batch-type AD experiment. The result from the batch-type reactor confirms the result obtained from the continuous-flow reactor. The cumulative methane from GL2 was 9039.69 mL/(g-VS), while at GL0.5, it was 262.83 mL/(g-VS). In the case of glucose, the overloaded reactor (GL0.5) ceased to produce methane on day 3, and the pH had reached 4.0. For FW, the cumulative methane for FW2 was 9452.42 mL/(g-VS), while FW0.5 was 5696.03 mL/(g-VS). The cumulative methane from the WS from both ISRs is close to each other, where at WS2, it was 5413.48 mL/(g-VS) while at WS0.5 it was 4900.67 mL/(g-VS), compared to FW and glucose, where overloading the reactor resulted in a significant decrease in methane production.

3.3 | Analysis of VFA Distribution

To complement the results of determining the total amount of volatile fatty acids (TFVAs), a detailed analysis was carried out to determine the distribution of the acids in the samples. VFA analysis was carried out using Ultra High-Performance Liquid Chromatography, and the results are shown in Figure 5. Higher VFAs (acetic and propionic) production was observed for the three tested substrates in reactors with an ISR of 0.5. At ISR2.0, only small amounts of propionic acid were detected at a few measurement points. On the last day of HRT (day 20), for ISR 2.0, a comparable amount of acetic acid was observed, which decreased by more than half at the

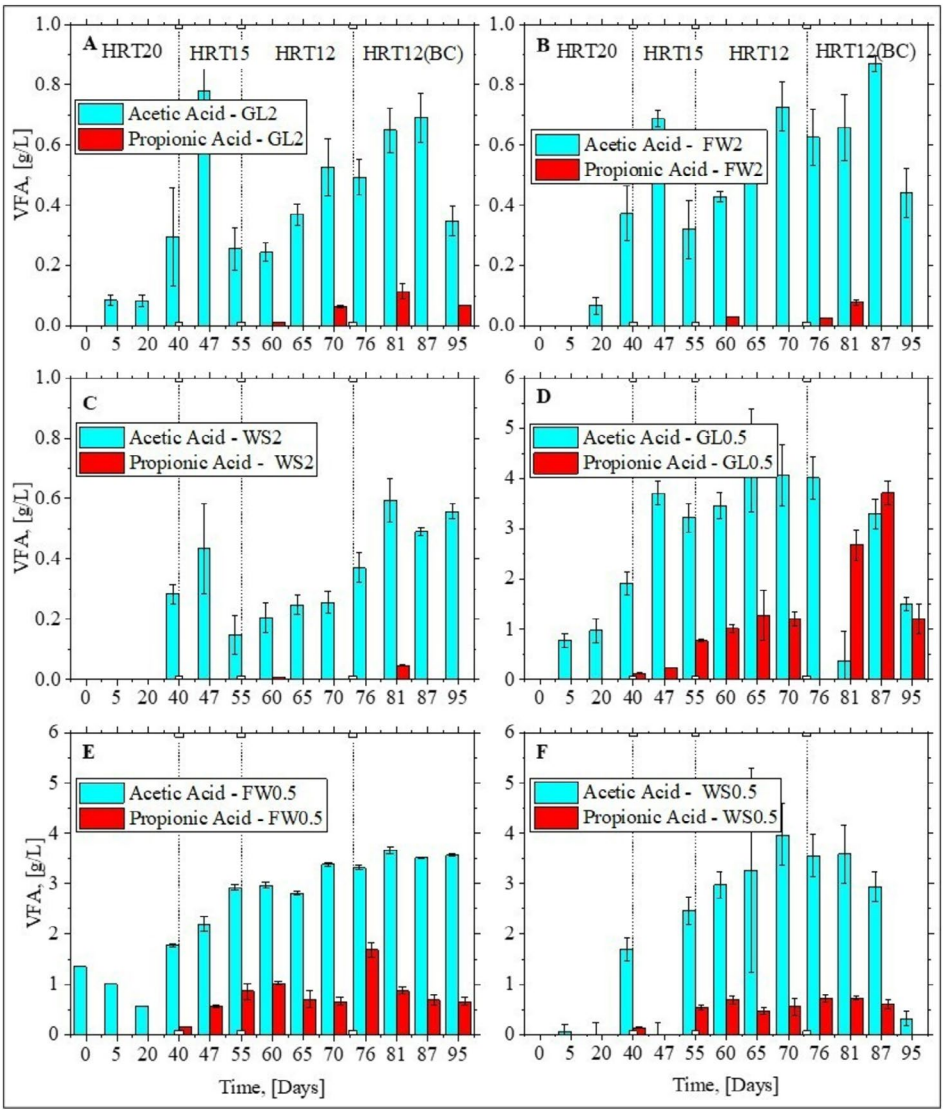

FIGURE 5 | Specific volatile fatty acid concentrations during fermentation. (A) reactor with glucose at ISR2, (B) food waste at ISR2, (C) wheat straw at ISR2, (D) glucose at ISR0.5, (E) food waste at ISR0.5, and (F) wheat straw at ISR0.5.

next measurement point for each of the reactors with ISR 2.0. At ISR0.5, both acetic and propionic acids were observed. As shown in Figure 5D, where ISR was 0.5, and glucose was the substrate, the highest concentration of acetic acid was measured at 4.35 g/L on day 65 of the experiment, corresponding to the midpoint of HRT 12. For this reactor, significant differences in the ratio of acetic to propionic acid were also observed in the final phase of the experiment, starting from day 76. This reactor also recorded the highest amount of propionic acid, which peaked at 3.71 g/L on day 87. For the reactor using FW at ISR0.5, the acetic acid level was maintained at a stable level from day 47 of the experiment, ranging from 2.19 g/L to a maximum of 3.67 g/L. In the reactor where WS was used as a substrate at ISR0.5 (Figure 5F), the acetic acid level remained similar throughout the experiment, with its highest amount recorded on day 70 (at the final phase of HRT12).

Application of more complex substrates such as FW and WS, which also had a variety of other nutrients in their composition, indicates that they preserve the process under more stable conditions of acetic to propionic acid ratio (ISR0.5). At the same time, similar amounts were released into the fermentation medium.

3.4 | Real-Time PCR and NGS

The qPCR results (ratios of the *mcr*A to 16S rRNA gene copy numbers) (Figure 6) illustrate the prevalence of the *mcr*A gene in the total microbial population. At HRT12, the gene copy numbers at GL2.0 and WS2.0 increased. In general, before the BC addition, the relative abundances of *mcr*A were higher at ISR2.0, indicating that overfeeding the reactors could suppress gene expression. It was previously shown that in AD of FW carried out at high OLRs, the highest relative abundance of *mcr*A, *mcr*B and *mcr*G genes was noted on the first day of the experiment (Zhao et al. 2021), suggesting the overloading of the system. Interestingly, during the BC phase, the relative abundance of *mcr*A increased significantly for WS0.5, indicating an enriched microbial community. This could explain the significant

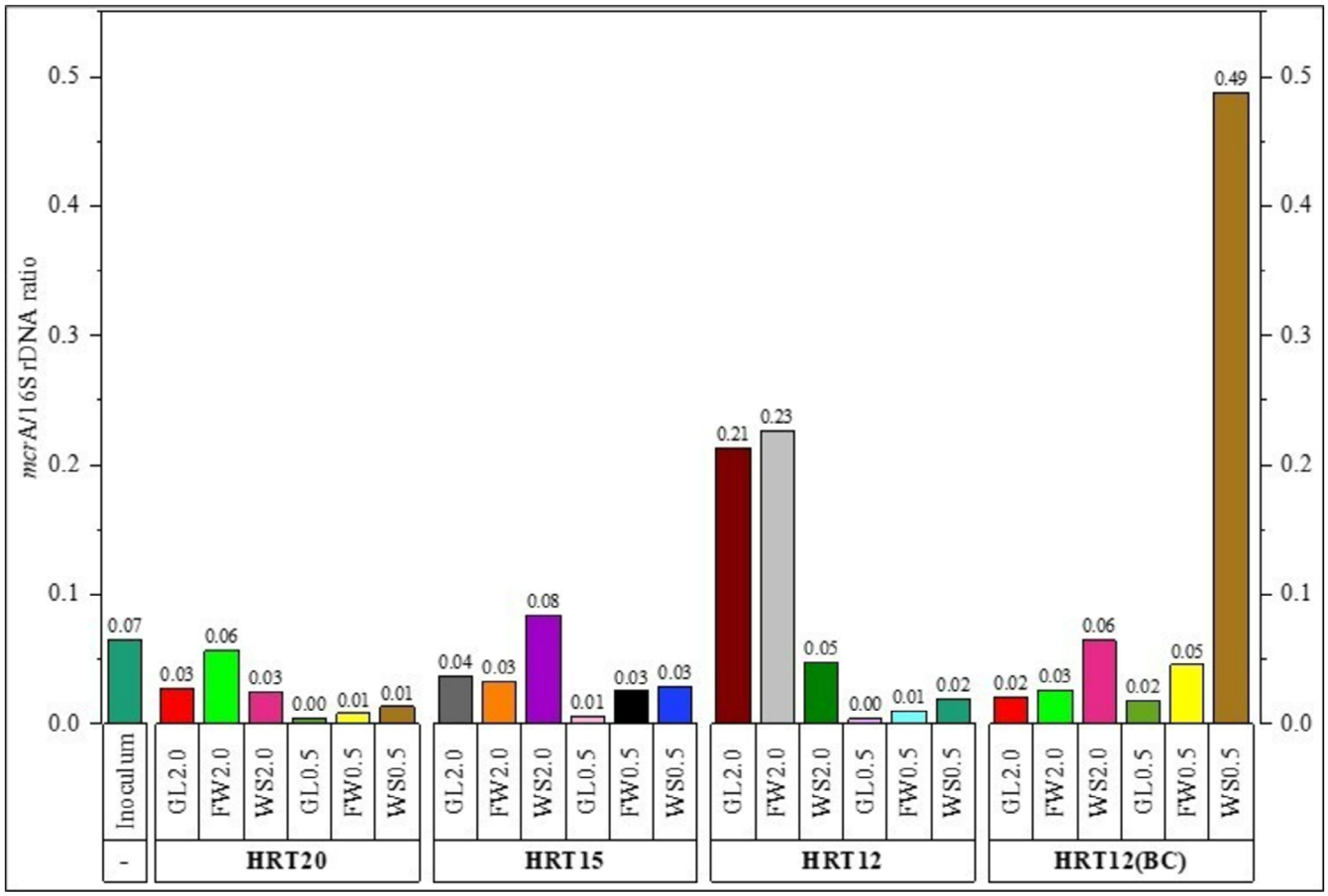

FIGURE 6 | Relative abundance of the *mcr*A gene in the microbiomes of each sample.

increase in the SMP (Figure 3A) and correlates with the shift in the archaeal microbial structure (Figure 8).

Regarding NGS results, alpha diversity indices (Shannon's index, observed features, and Pielou's Evenness) for bacteria and archaea are given in Tables S10 and S11, respectively. Shannon's index measures richness (the higher the number, the higher the diversity of species in a particular community); the observed features metric is simply the count of individual species (the higher the index, the greater the number of species); whereas Pielou's Evenness is in the range of 0–1 (where 0 signifies no evenness, and 1 a complete evenness). WS0.5 consistently maintained the highest bacterial diversity (Shannon index 4.8–5.4), followed by FW, with GL showing the lowest diversity (Shannon index as low as 0.5 for GL0.5) (Table S8).

Beta diversity quantifies dissimilarities among communities. In this paper, the Bray-Curtis metric, which considers not only presence and absence but also abundance, was employed. The results are presented in Supporting Information, Figures S12 and S13 for bacteria and Figures S15 and S16 for archaea, considering differences regarding ISR and substrate. Figures S15 and S16 demonstrate that archaeal communities are clustered primarily by substrate type. Regarding taxonomy, microbial communities of bacteria and archaea at the class (Figures S14 and S17) and family (Figures 7 and 8) levels are presented. BC's addition shifted the archaeal community structure at WS0.5.

Figure S14 shows that specific bacterial groups dominate different treatments. The bacterial community structures of G2.0, FW2.0, and FW0.5 were affected by BC addition. The substrate-specific microbial community in GL reactors shifted notably with ISR: Bacilli dominated under most conditions at ISR 0.5, while Clostridia prevailed at ISR 2.0. The WS and FW-fed reactors have similar community structures. When ISR is considered, the relative abundance of *Clostridia* decreased while *Bacteroidia* increased at ISR0.5. However, during BC addition, for WS0.5, opposite shifting was observed in which *Clostridia* increased while *Bacteroidia* decreased. When the WS was applied, consistent dominance of *Clostridia*, particularly at ISR 0.5, was observed, while more balanced communities with significant proportions of *Clostridia*, *Bacteroidia*, and other groups, reflecting its intermediate biodegradability, were observed in FW. Considering the ISR effect on communities, there is a clear differentiation in community structure.

4 | Discussion

4.1 | Anaerobic Digestion

The lowest conversion efficiency in GL0.5 was due to the acidification and overloading. Moderate conversion efficiency was observed from the FW-fed reactors at 54.66% from FW0.5 and 66.56% from FW2.0. The results show that, for FW and GL, the

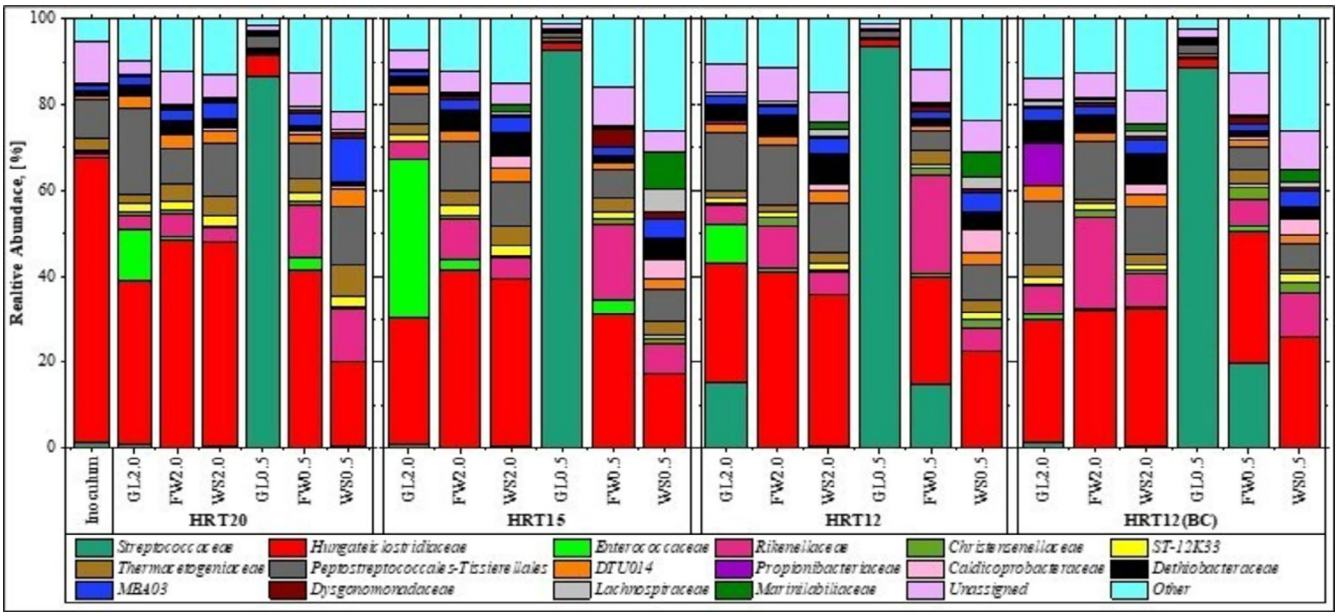

FIGURE 7 | Relative abundance of bacteria at the family level. 'Other' represents all taxons with relative abundance < 2%.

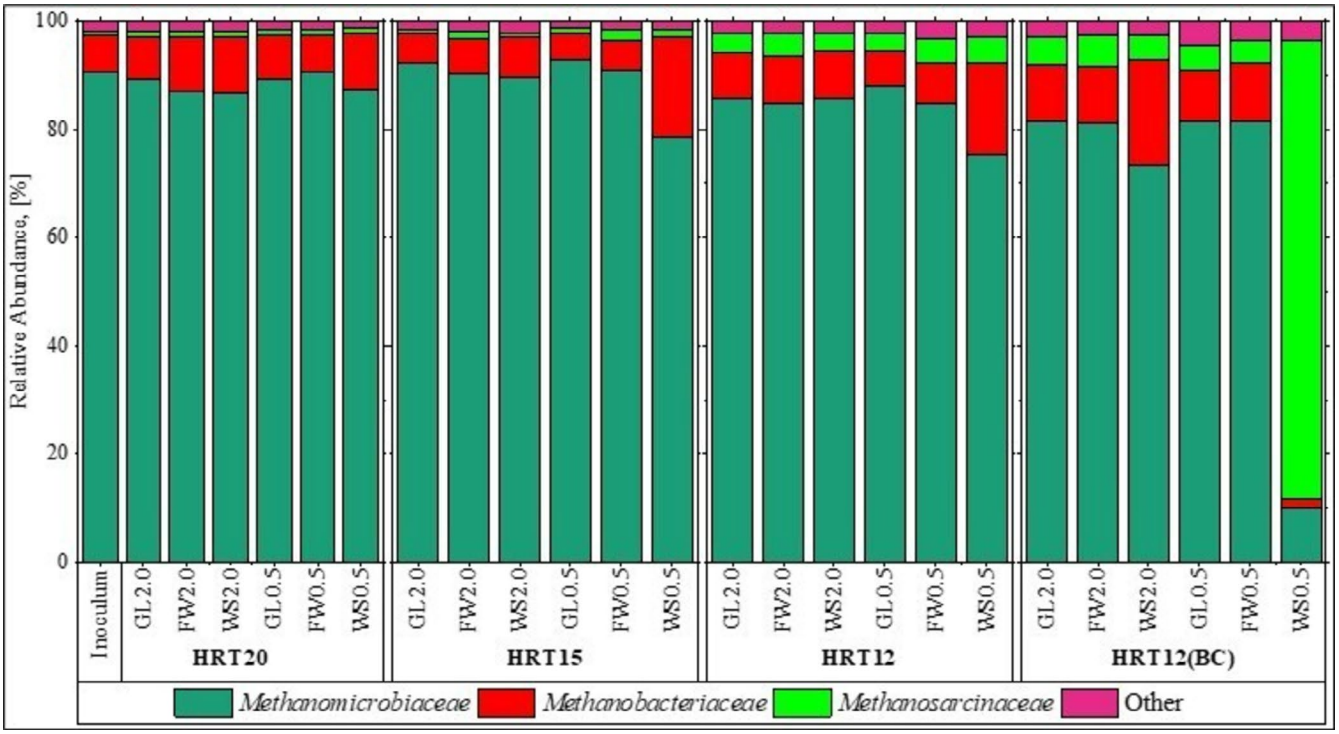

FIGURE 8 | Relative abundance of archaea at the family level. 'Other' represents all taxa with relative abundance < 2%.

ISR 2.0 favors biomethane production while increasing organic load decreases biomethane production in the case of FW or even breaks its production for GL. Additionally, the high C/N ratio of GL and FW could explain the high BMP under ISR2.0 (Pulgarín-Muñoz et al. 2025). WS is the only substrate that benefits from an increased organic load, showing that ISR should be adjusted depending on the biodegradability. This occurs because easily degradable substances (FW and GL) rapidly decompose, leading to acid accumulation that outpaces methanogen consumption and disrupts the reactor's pH balance. On the other hand, WS benefited at a high organic load because only a small portion was decomposed; thus, increasing the organic load increases available food for microorganisms, without accumulation of the intermediates.

In the case of FW0.5, the biomethane production stopped on day 2, plateauing until day 6 (Figure 2). After this period, the system recovered, showing a sharp increase in biomethane production, which then leveled off on day 21 and remained stable for the rest of the process. GL0.5 exhibited a cessation of biomethane production on day 2, while WS0.5 showed a gradual, continuous production throughout the process. This

suggests that overloading the reactor with highly biodegradable substrates can lead to system failure. However, when less biodegradable substrates like WS are used, the reactor can maintain biological activity at similar production levels when ISR is set to 2.0. At GL0.5, there is an excess of the substrate relative to the microorganisms, leading to rapid fermentation of GL, accompanied by an increase in the TVFA (9.70 g/L) (Table S4) and a decrease in pH from an initial value of 8.44 to 4.58. In contrast, WS is a more complex, lignocellulosic substrate that degrades slowly due to its lower biodegradability ($k = 0.0019\,\text{day}^{-1}$) (Table 2).

The behavior of the reactor fed with FW at ISR 0.5 can be explained by its intermediate biodegradability ($k = 0.002\,\text{day}^{-1}$) (Table 2). Like GL, FW is partially comprised of readily degradable organic materials, such as sugars, fats, and proteins, which can lead to rapid microbial consumption and the accumulation of VFAs. The high TVFA concentration of FW0.5 at 16.57 g/L on day 3 (Table S4), caused temporary acidification (pH dropped from 8.5 to 7.5 by day 3). As a result, the system experiences a decrease in biomethane production, which nearly halted on day 2. However, unlike GL, which is highly biodegradable and degrades almost immediately, FW contains more complex and slow-degradable components, such as fibrous materials. These components degrade more slowly, allowing the system to recover gradually after the initial acidification. Between days 2 and 6, the methanogenic microbes likely adjust and recover as the VFAs are slowly converted into methane, stabilizing the system's pH. The pattern of FW0.5—a lag phase followed by a sharp increase in biomethane production—indicates that the intermediate biodegradability of FW creates an initial overload of easily degradable substrates, but the slower-degrading components enable recovery and sustained biomethane production as the process progresses.

4.2 | Biochar's Metal Mobilization

When BC was added, the concentration of Cobalt (Co) and Nickel (Ni) increased at WS0.5 while Iron (Fe) remained relatively high (Table S3). These metals act as cofactors in essential enzymes such as the Acetyl-CoA Synthase (ACS) (Sugiarto et al. 2021) and methyl-coenzyme M reductase (MCR) (Sánchez et al. 2021) that catalyze the chemical reactions needed to produce CH_4 during methanogenesis. The ACS enzyme uses Ni and Fe to convert acetate to CH_4. Iron supports electron transfer reactions essential for energy generation during methanogenesis (Sugiarto et al. 2021). Therefore, it could be assumed that BC addition improved the system by providing essential enzyme cofactors.

The oxygen content in the non-biochar phase varies between 31.61% and 43.58%, whereas in the biochar supplementation phase, it ranges from 25.93% to 36.47%. The reduction in oxygen content in BC samples aligns with findings from previous studies, where biochar amendment leads to decreased oxidation and improved nutrient retention (Liu et al. 2017). Furthermore, an increase in C content from approximately 22%–28% in non-BC samples to 38%–57% in BC samples corroborates the role of biochar in enhancing organic matter stabilization.

The biochar-amended samples also show a notable decrease in lead concentration, indicating possible heavy metal immobilization. This is consistent with research showing the potential of biochar to adsorb heavy metals, reducing their bioavailability (Beesley et al. 2011; Xu et al. 2013). Another significant finding is the decrease in Cl concentration from 6.32%–11.75% (non-BC) to 2.38%–7.24% (with BC), since biochar-amended systems are known to reduce chloride leaching, improving the quality of the soil and digestate (Ahmad et al. 2014). The results suggest that biochar supplementation significantly improved the physicochemical properties of digestate by enhancing nutrient retention, stabilizing organic matter, and reducing heavy metal bioavailability. These findings align with previous research that highlights the benefits of biochar in agricultural waste management, particularly for its potential to enhance soil fertility and mitigate environmental contamination (Ren et al. 2018).

4.3 | Analysis of VFA Distribution

Butyric acid was not observed in any sample. The absence of butyric acid may be affected by several factors that indicate specific conditions or microbial activities within the fermentation system that favor the production of other VFAs over butyric acid. The observed phenomena are related to a lack of butyrate-producing strains, from which *Clostridium butyricum* and other microbial communities from dark fermentation convert substrates lactate to acetate and butyrate (Detman et al. 2019).

The results obtained correlated with biogas production and agree with previous reports in this aspect. Higher levels of propionic acid compared to acetic acid in methane fermentation affect biomethane production and indicate a change in the dynamics of the process (Feng et al. 2009; Suwannakham and Yang 2005). The ratio of acetic acid to propionic acid plays an important role in the biogas production process since propionic acid fermentation uses electrons, which reduces biomethane production (Feng et al. 2009). The research also suggests that propionate synthesis during carbohydrate fermentation can sequester hydrogen, thus reducing its availability for biomethane production by methanogenic bacteria (Liang et al. 2012). The results obtained during the experiment indicate this, as when glucose was used as a substrate, the highest concentrations of propionate were observed. At the same time, it had a higher proportion of acetic acid, and this was correlated with lower biomethane production.

A higher proportion of propionic acid compared to acetic acid in biomethane fermentation processes could potentially lead to reduced methane production due to the use of hydrogen in propionate synthesis and other mechanisms that affect the overall fermentation process. The higher rates of propionic acid compared to acetic acid negatively affected biomethane production. That agrees with the theory that propionate synthesis can sequester hydrogen, reducing its availability to methanogenic bacteria. More complex substrates (FW and WS) allowed the acetic acid/propionic acid ratio to remain more stable at an ISR of 0.5, resulting in better methane production compared to glucose. A higher ISR (2.0) promoted more efficient conversion of substrates to biomethane, probably due to a better balance of microbial populations and reduced accumulation of process inhibitors such as excess VFAs. Overall, the results indicate that

the ISR and the type of substrate play an important role in optimizing the methane fermentation process. Higher ISR generally promotes higher biomethane production and process stability, especially for more difficult-to-degrade substrates such as WS.

4.4 | Real-Time PCR and NGS

Lower ISR (0.5) treatments showed more extreme diversity patterns—either very high (WS0.5) or very low (GL0.5)—suggesting that higher organic loading creates more selective pressure. The archaeal diversity (Table S11) shows an overall lower diversity compared to bacteria (Shannon index 0.6–1.5). It indicates a gradual increase in diversity over time in most treatments.

At ISR 2.0, more diverse communities with higher proportions of various bacterial classes were observed, while at ISR 0.5, more specialized communities, particularly for GL0.5 (*Bacilli*-dominated) and WS0.5 (*Clostridia*-dominated), were observed. *Clostridia* and *Bacilli* were reported to produce acetate (Ma et al. 2017), which is consistent with the results obtained in this study (Figure 5). *Clostridia* were reported to degrade solid (Pan et al. 2019), which could explain their lower abundance in GL0.5 with lower solid contents compared to reactors with higher solid contents. The *Bacteroidia* increased their abundance at HRT 15 and HRT 12, corresponding to increased OLR (Pan et al. 2019).

BC supplementation showed significant variation in the community. With GL2.0, BC addition increased the relative abundance of *Actinobacteria* and decreased the relative abundance of *Clostridia* and *Bacteroidia*, while *Bacilli* stayed more or less the same. *Clostridia* include many syntrophic bacteria that work effectively with methanogens in digesting complex substrates. The extreme dominance of *Bacilli* in GL0.5 correlates with its high VFA accumulation and process instability—the community was likely too specialized in fermentation without sufficient VFA consumers. The BC-induced archaeal community shifts, particularly the increased diversity in WS0.5, demonstrate biochar's role as a habitat provider that promotes a more balanced microbial community, probably due to its properties such as high surface area (32.94 cm^2/g) or buffering capacity. The more gradual changes observed in WS treatments across different HRTs explain their greater stability compared to the rapidly shifting GL communities. This microbial community data provides mechanistic evidence for why substrate biodegradability interacts so significantly with ISR and BC effects, with the most beneficial BC impact occurring in the WS0.5 condition, where it promoted a more balanced microbial community better adapted to the slower degradation of lignocellulosic material.

Overall, the community shift resulting from BC addition explains why this treatment showed the most significant improvement in methane production with BC (increasing from 100.10 to 140.70 mL/(g-VS)). The diverse community likely provided metabolic resilience. On the other hand, the process inhibition in GL0.5 showed extremely low bacterial diversity in GL0.5 (Shannon index 0.5–0.9, a strong Bacilli dominance), which correlates with the high VFA accumulation and process instability observed. The rapid degradation of glucose likely created selective pressure for acidogenic bacteria while inhibiting methanogens. The intermediate stability of FW-fed reactors was observed, giving moderate community diversity, which aligns with its intermediate biodegradability and partial recovery after initial acidification in batch tests.

The microbial data suggest that BC mechanisms were more focused on providing attachment surfaces that support more diverse communities. BC potentially adsorbs inhibitory compounds (as seen in VFA reduction in WS0.5). Furthermore, the BC created microhabitats that fostered syntrophic relationships between bacteria and methanogens.

The microbial analysis provides critical mechanistic explanations for the varying responses to ISR and BC across substrate types. Substrate biodegradability dictates initial community selection and adaptation potential. Lower ISR creates stronger selective pressure, beneficial only when the substrate degradation rate matches microbial adaptation capacity (as in WS0.5). BC provides the most benefit in systems where microbial communities are diverse but stressed (WS0.5). Interestingly, it was recently proven that other abiotic additives, such as clinoptilolite, alter significantly the composition of the microbial communities in anaerobic co-digestion of sewage sludge, citrus waste, and brewery spent grain (Szaja et al. 2025), while granular activated carbon was demonstrated to enrich *Synergistes* and *Geobacter*, as well as *Methanolinea* and *Methanosaeta* during AD of dairy wastewaters (Logan et al. 2022). Likewise, magnetic BC and nanoparticles were proven to affect methane production via direct interspecies electron transfer or stimulating microorganisms to metabolize VFAs (Al-Essa et al. 2024; Gao et al. 2022).

4.5 | Summary

The experiment arrived with significant findings for batch and continuous AD tests. The results revealed that a lower ISR positively influenced the degradation of substrates, resulting in higher biomethane production. BC supplementation enhanced the biomethane production of the hardly biodegradable substrate (WS), probably due to releasing trace elements (Ni Co) serving as enzyme cofactors. The potential role of BC in the adsorption of AD inhibitors, such as VFA, and as the provider of protective habitat for stressed microbial communities, was also observed in this study. Furthermore, BC addition shifted the bacterial community to a more diverse and balanced community.

Author Contributions

Marvin T. Valentin: writing – Original draft, Writing – Reviewing and Editing, Conceptualization, Methodology, Data analysis and interpretation. **Katarzyna Ewa Kosiorowska:** resources, software, writing – review and editing. **Agata Siedlecka:** software, supervision, validation, writing – review and editing. **Kacper Świechowski:** resources, validation, writing – review and editing. **Vitalii Demeshkant:** resources, writing – review and editing. **Paweł Wiercik:** resources, writing – review and editing. **Svetlana Ashikhmina:** resources. **Tomasz Strzała:** resources, software, visualization, writing – review and editing. **Andrzej Białowiec:** conceptualization, Writing – Reviewing and Editing, Supervision and Funding acquisition.

Acknowledgements

The article is part of a PhD dissertation titled 'Enhancement of Biomethane Production from Biomass by the Addition of Biochar', prepared during the Doctoral School at the Wrocław University of Environmental and Life Sciences.

Conflicts of Interest

The authors declare no conflicts of interest.

Data Availability Statement

All data will be available in the form of a dataset submitted to the Knowledge Base repository of Wrocław University of Environmental and Life Sciences. The raw data are availabele under this DOI number: https://doi.org/10.57755/jbv7-5t65.

References

Ahmad, M., A. U. Rajapaksha, J. E. Lim, et al. 2014. "Biochar as a Sorbent for Contaminant Management in Soil and Water: A Review." *Chemosphere* 99: 19–33. https://doi.org/10.1016/j.chemosphere.2013.10.071.

Al-Essa, E. M., R. Bello-Mendoza, and D. G. Wareham. 2024. "Interaction Between Magnetite and Inoculum Characteristics in Accelerating Methane Production Kinetics." *GCB Bioenergy* 16: 1–14. https://doi.org/10.1111/gcbb.13189.

Aydin, S., B. Ince, and O. Ince. 2015. "Application of Real-Time PCR to Determination of Combined Effect of Antibiotics on Bacteria, Methanogenic Archaea, Archaea in Anaerobic Sequencing Batch Reactors." *Water Research* 76: 88–98. https://doi.org/10.1016/j.watres.2015.02.043.

Beesley, L., E. Moreno-Jiménez, J. L. Gomez-Eyles, E. Harris, B. Robinson, and T. Sizmur. 2011. "A Review of Biochars' Potential Role in the Remediation, Revegetation and Restoration of Contaminated Soils." *Environmental Pollution* 159: 3269–3282. https://doi.org/10.1016/j.envpol.2011.07.023.

Benito, P. C., and M. Greger. 2017. "Influence of the Substrate/Inoculum Ratio on Process Stability and Performance During Batch Digestion of Grass Silage." *Chemie-Ingenieur-Technik* 89: 724–732. https://doi.org/10.1002/cite.201600008.

Białowieca, A., and E. Syguła. 2025. "Carbon-Relative Molar Mass Is a New Parameter for Experimentation With Different Biomasses. Prediction of Higher Heating Value Case Study."

Buswell, A. M., and H. F. Mueller. 1952. "Mechanism of Methane Fermentation." *Industrial and Engineering Chemistry* 44: 550–552. https://doi.org/10.1021/ie50507a033.

Cai, J., P. He, Y. Wang, L. Shao, and F. Lü. 2016. "Effects and Optimization of the Use of Biochar in Anaerobic Digestion of Food Wastes." *Waste Management & Research* 34: 409–416. https://doi.org/10.1177/0734242X16634196.

Chakraborty, D., O. P. Karthikeyan, A. Selvam, S. G. Palani, M. M. Ghangrekar, and J. W. C. Wong. 2022. "Two-Phase Anaerobic Digestion of Food Waste: Effect of Semi-Continuous Feeding on Acidogenesis and Methane Production." *Bioresource Technology* 346: 126396. https://doi.org/10.1016/j.biortech.2021.126396.

Czekała, W., T. Jasiński, M. Grzelak, K. Witaszek, and J. Dach. 2022. "Biogas Plant Operation: Digestate as the Valuable Product." *Energies* 15: 1–11. https://doi.org/10.3390/en15218275.

den Boer, J., P. Kobel, E. den Boer, and G. Obersteiner. 2023. "Food Waste Quantities and Composition in Polish Households." *Waste Management & Research* 41: 1318–1330. https://doi.org/10.1177/0734242X231155095.

Detman, A., D. Mielecki, A. Chojnacka, A. Salamon, and M. K. Błaszczyk. 2019. "Cell Factories Converting Lactate and Acetate to Butyrate: Clostridium Butyricum and Microbial Communities From Dark Fermentation Bioreactors." *Microbial Cell Factories* 18: 1–12. https://doi.org/10.1186/s12934-019-1085-1.

Elliott, J. A. K., C. Krohn, and A. S. Ball. 2024. "Source-Separated Industrial Wastewater Is a Candidate for Biogas Production Through Anaerobic Digestion." *Fermentation* 10: 10. https://doi.org/10.3390/fermentation10030165.

Feng, L., Y. Chen, and X. Zheng. 2009. "Enhancement of Waste Activated Sludge Protein Conversion and Volatile Fatty Acids Accumulation During Waste Activated Sludge Anaerobic Fermentation by Carbohydrate Substrate Addition: The Effect of pH." *Environmental Science & Technology* 43: 4373–4380. https://doi.org/10.1021/es8037142.

Gao, M., P. Du, B. Zhi, et al. 2022. "Magnetic Biochar Affects the Metabolic Pathway in Methanogenesis of Anaerobic Digestion of Food Waste." *GCB Bioenergy* 14: 572–584. https://doi.org/10.1111/gcbb.12931.

IEA Bioenergy. 2018. "Value of Batch Tests for Biogas Potential Analysis."

Johnravindar, D., R. Kumar, L. Luo, et al. 2022. "Influence of Inoculum-To-Substrate Ratio on Biogas Enhancement During Biochar-Assisted Co-Digestion of Food Waste and Sludge." *Environmental Technology (United Kingdom)*: 1–13. https://doi.org/10.1080/09593330.2022.2161949.

Liang, Z. X., L. Li, S. Li, Y. H. Cai, S. T. Yang, and J. F. Wang. 2012. "Enhanced Propionic Acid Production From Jerusalem Artichoke Hydrolysate by Immobilized *Propionibacterium acidipropionici* in a Fibrous-Bed Bioreactor." *Bioprocess and Biosystems Engineering* 35: 915–921. https://doi.org/10.1007/s00449-011-0676-y.

Liu, T., X. Zhou, Z. Li, X. Wang, and J. Sun. 2019. "Effects of Liquid Digestate Pretreatment on Biogas Production for Anaerobic Digestion of Wheat Straw." *Bioresource Technology* 280: 345–351. https://doi.org/10.1016/j.biortech.2019.01.147.

Liu, Z., B. Dugan, C. A. Masiello, and H. M. Gonnermann. 2017. "Biochar Particle Size, Shape, and Porosity Act Together to Influence Soil Water Properties." *PLoS One* 12: 1–19. https://doi.org/10.1371/journal.pone.0179079.

Logan, M., L. C. Tan, C. O. Nzeteu, and P. N. L. Lens. 2022. "Enhanced Anaerobic Digestion of Dairy Wastewater in a Granular Activated Carbon Amended Sequential Batch Reactor." *GCB Bioenergy* 14: 840–857. https://doi.org/10.1111/gcbb.12947.

Ma, H., H. Liu, L. Zhang, M. Yang, B. Fu, and H. Liu. 2017. "Novel Insight Into the Relationship Between Organic Substrate Composition and Volatile Fatty Acids Distribution in Acidogenic Co-Fermentation." *Biotechnology for Biofuels* 10: 1–15. https://doi.org/10.1186/s13068-017-0821-1.

Maeda, H., C. Fujimoto, Y. Haruki, et al. 2003. "Quantitative Real-Time PCR Using TaqMan and SYBR Green for *Actinobacillus actinomycetemcomitans*, *Porphyromonas gingivalis*, *Prevotella intermedia*, tetQ Gene and Total Bacteria." *FEMS Immunology and Medical Microbiology* 39: 81–86. https://doi.org/10.1016/S0928-8244(03)00224-4.

Matoute, A., S. Maestri, M. Saout, et al. 2024. "Meat-Borne-Parasite: A Nanopore-Based Meta-Barcoding Work-Flow for Parasitic Microbiodiversity Assessment in the Wild Fauna of French Guiana." *Current Issues in Molecular Biology* 46: 3810–3821. https://doi.org/10.3390/cimb46050237.

Molatudi, L. E., T. J. Kunene, and T. Mashifana. 2025. "Strategies for Biomethane Purification: A Critical Review and New Approaches." *GCB Bioenergy* 17: 17. https://doi.org/10.1111/gcbb.70040.

Nagao, N., N. Tajima, M. Kawai, et al. 2012. "Maximum Organic Loading Rate for the Single-Stage Wet Anaerobic Digestion of Food Waste." *Bioresource Technology* 118: 210–218. https://doi.org/10.1016/j.biortech.2012.05.045.

Namal, O. O. 2020. "Investigation of the Effects of Different Conductive Materials on the Anaerobic Digestion." *International Journal of Environmental Science and Technology* 17: 473–482. https://doi.org/10.1007/s13762-019-02498-x.

Ngo, T., L. S. Khudur, S. Hassan, K. Jansriphibul, and A. S. Ball. 2024. "Enhancing Microbial Viability With Biochar for Increased Methane Production During the Anaerobic Digestion of Chicken Manure." *Fuel* 368: 131603. https://doi.org/10.1016/j.fuel.2024.131603.

Nguyen, D. D., B. H. Jeon, J. H. Jeung, et al. 2019. "Thermophilic Anaerobic Digestion of Model Organic Wastes: Evaluation of Biomethane Production and Multiple Kinetic Models Analysis." *Bioresource Technology* 280: 269–276. https://doi.org/10.1016/j.biortech.2019.02.033.

Pan, J., J. Ma, L. Zhai, and H. Liu. 2019. "Enhanced Methane Production and Syntrophic Connection Between Microorganisms During Semi-Continuous Anaerobic Digestion of Chicken Manure by Adding Biochar." *Journal of Cleaner Production* 240: 118178. https://doi.org/10.1016/j.jclepro.2019.118178.

Pererva, Y., C. D. Miller, and R. C. Sims. 2020. "Existing Empirical Kinetic Models in Biochemical Methane Potential (BMP) Testing, Their Selection and Numerical Solution." *Water* 12: 216–218. https://doi.org/10.1093/acprof:oso/9780195371833.003.0024.

Pulgarín-Muñoz, C. E., J. C. Saldarriaga-Molina, J. C. Castro-Valencia, M. A. Correa-Ochoa, and J. D. Echeverry-Ruiz. 2025. "Effect of the Co-Substrate Ratio on the Anaerobic Co-Digestion of Sewage Sludge and the Organic Fraction of Municipal Solid Waste at Pilot Scale." *International Biodeterioration & Biodegradation* 198: 106008. https://doi.org/10.1016/j.ibiod.2025.106008.

Ren, X., G. Zeng, L. Tang, et al. 2018. "Effect of Exogenous Carbonaceous Materials on the Bioavailability of Organic Pollutants and Their Ecological Risks." *Soil Biology and Biochemistry* 116: 70–81. https://doi.org/10.1016/j.soilbio.2017.09.027.

Romio, C., M. Vedel Wegener Kofoed, and H. Bjarne Møller. 2022. "Effect of Ultrasonic and Electrokinetic Post-Treatments on Methane Yield and Viscosity of Agricultural Digestate." *Bioresource Technology* 358: 127388. https://doi.org/10.1016/j.biortech.2022.127388.

Sánchez, E., C. Herrmann, W. Maja, and R. Borja. 2021. "Effect of Organic Loading Rate on the Anaerobic Digestion of Swine Waste With Biochar Addition." *Environmental Science and Pollution Research* 28: 38455–38465. https://doi.org/10.1007/s11356-021-13428-1.

Shao, Z., Q. Fan, F. Gao, et al. 2025. "Sustained Methane Production Enhancement by Magnetic Biochar and Its Recovery in Semi-Continuous Anaerobic Digestion With Varying Substrate C/N Ratios." *Chemical Engineering Journal* 514: 1–8. https://doi.org/10.1016/j.cej.2025.163050.

Sugiarto, Y., N. M. S. Sunyoto, M. Zhu, I. Jones, and D. Zhang. 2021. "Effect of Biochar Addition on Microbial Community and Methane Production During Anaerobic Digestion of Food Wastes: The Role of Minerals in Biochar." *Bioresource Technology* 323: 124585. https://doi.org/10.1016/j.biortech.2020.124585.

Suwannakham, S., and S. T. Yang. 2005. "Enhanced Propionic Acid Fermentation by *Propionibacterium acidipropionici* Mutant Obtained by Adaptation in a Fibrous-Bed Bioreactor." *Biotechnology and Bioengineering* 91: 325–337. https://doi.org/10.1002/bit.20473.

Szaja, A., A. Montusiewicz, A. Cydzik-Kwiatkowska, S. Pasieczna-Patkowska, and M. Lebiocka. 2025. "Enhancing Methane Production Through co-Digestion of Sewage Sludge, Citrus Waste and Brewery Spend Grain With Natural Zeolite: Mechanisms and Microbiome Analysis." *GCB Bioenergy* 17: 17. https://doi.org/10.1111/gcbb.70029.

Torquato, L. D. M., P. M. Crnkovic, C. A. Ribeiro, and M. S. Crespi. 2017. "New Approach for Proximate Analysis by Thermogravimetry Using CO_2 Atmosphere: Validation and Application to Different Biomasses." *Journal of Thermal Analysis and Calorimetry* 128: 1–14. https://doi.org/10.1007/s10973-016-5882-z.

Valentin, M. T., and A. Białowiec. 2024a. "Influence of Inoculum-To-Substrate Ratio on Biomethane Production via Anaerobic Digestion of Biomass." *Environmental Microbiology Reports* 16: 1–14. https://doi.org/10.1111/1758-2229.70009.

Valentin, M. T., and A. Białowiec. 2024b. "Impact of Using Glucose as a Sole Carbon Source to Analyze the Effect of Biochar on the Kinetics of Biomethane Production." *Scientific Reports* 14: 1–10. https://doi.org/10.1038/s41598-024-59313-y.

Valentin, M. T., K. Świechowski, and A. Białowiec. 2023. "Influence of Pre-Incubation of Inoculum With Biochar on Anaerobic Digestion Performance." *Materials (Basel)* 16: 1–13. https://doi.org/10.3390/ma16206655.

van Meerbeek, K., L. Appels, R. Dewil, et al. 2014. "Energy Potential for Combustion and Anaerobic Digestion of Biomass From Low-Input High-Diversity Systems in Conservation Areas." *Global Change Biology. Bioenergy* 7: 1–16.

Wambugu, C. W., E. R. Rene, J. van de Vossenberg, C. Dupont, and E. D. van Hullebusch. 2019. "Role of Biochar in Anaerobic Digestion Based Biorefinery for Food Waste." *Frontiers in Energy Research* 7: 1–13. https://doi.org/10.3389/fenrg.2019.00014.

Xiao, Y., F. Zan, W. Zhang, and T. Hao. 2022. "Alleviating Nutrient Imbalance of Low Carbon-To-Nitrogen Ratio Food Waste in Anaerobic Digestion by Controlling the Inoculum-To-Substrate Ratio." *Bioresource Technology* 346: 126342. https://doi.org/10.1016/j.biortech.2021.126342.

Xu, X., X. Cao, L. Zhao, H. Wang, H. Yu, and B. Gao. 2013. "Removal of cu, Zn, and cd From Aqueous Solutions by the Dairy Manure-Derived Biochar." *Environmental Science and Pollution Research* 20: 358–368. https://doi.org/10.1007/s11356-012-0873-5.

Zhang, B., G. Wang, X. Zhang, et al. 2024. "Regulatory Mechanisms of Biochar Alleviating Ammonia Inhibition to Methanogenesis During Long-Term Operation of Anaerobic Membrane Bioreactor Treating Swine Wastewater." *Chemical Engineering Journal* 493: 1–7. https://doi.org/10.1016/j.cej.2024.152591.

Zhao, W., H. Yang, S. He, Q. Zhao, and L. Wei. 2021. "A Review of Biochar in Anaerobic Digestion to Improve Biogas Production: Performances, Mechanisms and Economic Assessments." *Bioresource Technology* 341: 125797. https://doi.org/10.1016/j.biortech.2021.125797.

Zheng, H., Z. Wang, X. Deng, et al. 2013. "Characteristics and Nutrient Values of Biochars Produced From Giant Reed at Different Temperatures." *Bioresource Technology* 130: 463–471. https://doi.org/10.1016/j.biortech.2012.12.044.

Supporting Information

Additional supporting information can be found online in the Supporting Information section. **Data S1:** gcbb70090-sup-0001-Supinfo.docx.